

Collisional unfolding of multiprotein complexes reveals cooperative stabilization upon ligand binding

Shuai Niu and Brandon T. Ruotolo*

Department of Chemistry, University of Michigan, Ann Arbor, Michigan 48109

Received 28 March 2015; Accepted 29 April 2015

DOI: 10.1002/pro.2699

Published online 13 May 2015 proteinscience.org

Abstract: Cooperative binding mechanisms are a common feature in biology, enabling a diverse range of protein-based molecular machines to regulate activities ranging from oxygen uptake to cellular membrane transport. Much, however, is not known about such cooperative binding mechanisms, including how such events typically add to the overall stability of such protein systems. Measurements of such cooperative stabilization events are challenging, as they require the separation and resolution of individual protein complex bound states within a mixture of potential stoichiometries to individually assess protein stabilities. Here, we report ion mobility-mass spectrometry results for the concanavalin A tetramer bound to a range of polysaccharide ligands. We use collision induced unfolding, a relatively new methodology that functions as a gas-phase analog of calorimetry experiments in solution, to individually assess the stabilities of concanavalin A bound states. By comparing the differences in activation voltage required to unfold different concanavalin A–ligand stoichiometries, we find evidence suggesting a cooperative stabilization of concanavalin A occurs upon binding most carbohydrate ligands. We critically evaluate this observation by assessing a broad range of ligands, evaluating the unfolding properties of multiple protein charge states, and by comparing our gas-phase results with those obtained from calorimetry experiments carried out in solution.

Keywords: mass spectrometry; ion mobility; collision induced dissociation; carbohydrate binding

Introduction

Protein biochemistry is replete with binding and interaction mechanisms that rely upon cooperativity, which acts as a form of general control to drive protein–ligand selectivity and function in many higher-order complexes.^{1–3} Beyond well-studied systems, such as the cooperative mechanism surrounding the binding of molecular oxygen and other ligands to hemoglobin,^{2,4} many additional proteins and protein

complexes have been identified that exhibit cooperative ligand binding mechanisms. For example, many protein–DNA complexes have well-known cooperative binding mechanisms that functionally regulate DNA replication.^{5,6} In addition, many protein-based motors and pumps rely upon cooperative binding of lipids and other small molecules to allosterically control protein function.⁷ While many questions remain surrounding the details of cooperative protein–ligand interactions *in vitro* and *in vivo*,⁸ a combination of theoretical models of protein–ligand binding cooperativity,^{9,10} in combination with detailed measurements of binding thermodynamics,¹¹ have been used to describe the functional consequences of a broad range of protein–ligand complexes.^{12,13}

In contrast to our understanding of protein–ligand binding cooperativity, detailed mechanisms that describe cooperative increases in protein

Additional Supporting Information may be found in the online version of this article.

Grant sponsors: National Science Foundation (B.T.R., CAREER Award, 1253384); and American Society for Mass Spectrometry (B.T.R., Research Award).

*Correspondence to: Brandon T. Ruotolo, Department of Chemistry, University of Michigan, 930 N. University Ave., Ann Arbor, MI 48109. E-mail: bruotolo@umich.edu

stability as a function such ligand binding events remain relatively elusive. For many years, cooperative effects have been invoked to describe enhancements to protein stability upon folding.¹¹ Computational chemistry approaches, for example, have been used to analyze the detailed cascade of noncovalent interactions, hydrogen bonds, and salt-bridges that give rise to folded structures and have identified cooperative elements in many cases.^{14–18} Similar examples centering on the protein stability acquired upon ligand binding are rare, but several have been reported.^{15,19–22} For example, density functional and *ab initio* methods in combination with molecular modeling have been used to quantify the hydrogen-bonding cooperativity in the context of biotin–avidin binding to be on the order of 4 kcal/mol.²³ Computational efforts dominate this area of research, as measurements of cooperative protein–ligand stabilization energies are tremendously challenging, beginning with the difficulties associated with recording evidence of cooperative binding patterns.^{10,18,24} Calorimetry data can, in principle, be analyzed to determine Hill coefficients which quantify the relative cooperativity of binding observed in experimental data, but such analyses are often difficult to execute, especially for large multiprotein systems, and dependent upon overall ligand concentration.^{4,25,26} To assess stability shifts for such systems, the separation of individual bound states of the biomolecules is required, which is often not possible using conventional spectroscopic or chromatographic techniques. These difficulties have resulted in a general dearth of experimental evidence for cooperative stabilization effects in proteins upon ligand binding.

Gas-phase structural biology methods, primarily based on nano-electrospray ionization (nESI) mass spectrometry (MS), possess the separation resolution and information content sufficient to address many of the challenges associated with the assessment of protein–ligand cooperativity and stability described above. MS methods can detect protein–ligand complexes,^{27–29} either intact or indirectly through mass shifts associated with chemical labeling,^{29–31} and have been used broadly to assess protein–ligand dissociation constants (K_D) and stability shifts in protein–ligand complexes.^{32–36} Recently, global methods, based on radical labeling and hydrogen deuterium exchange have been developed, capable of the *in vivo* assessment of protein–ligand binding and stability shifts throughout an entire proteome.³⁷ Similarly, MS of intact protein–ligand complexes has been used to resolve individual binding stoichiometries of small molecule ligands on large multiprotein targets, including the individual adenosine triphosphate (ATP) binding states of the 800 kDa GroEL chaperone assembly.^{22,38,39} In the most recent of these studies, MS was used to assess the

cooperativity of ATP binding to GroEL, demonstrating a strong fit to the Monod–Wyman–Changeux model of cooperativity, which preserves the symmetry of the protein–ligand states created.^{40,41}

In addition to quantifying the bound states within complex multiprotein–ligand systems, MS can also act to isolate protein complexes for stability measurements in the gas phase, following collisional activation. Such collision induced unfolding (CIU) experiments were first described for small monomeric protein ions⁴² but have rapidly expanded to include more detailed instrumentation⁴³ and applications covering large multiprotein complexes.^{35,44,45} To track gas-phase protein unfolding, MS must typically be coupled with ion mobility (IM), which acts to separate protein ions according to their orientationally averaged size and charge.⁴⁶ For example, CIU results have been used to record the gas-phase folding landscape of ubiquitin ions over a range of charge states using tandem IM instrumentation, with collisional activation regions between IM stages.⁴⁷ Additionally, CIU of protein complexes has measured the stability of salt-adducted assemblies,^{48,49} been used to assess stability enhancements in pathogenic mutants,³⁵ and differentiate conformationally selective kinase inhibitors.⁵⁰ Most recently, IM-MS and CIU data have been used to ascertain the selectivity and stability of bound lipids within the mechanosensitive channel of large conductance from *Mycobacterium tuberculosis*, as well as *E. coli* aquaporin and ammonia channels.⁴⁴

Here we apply CIU and MS measurements to capture cooperative increases in protein stability as a function of ligand attachment in a multiprotein–ligand binding system. Our target system is concanavalin A (Con A), a 103 kDa lectin tetramer that has been well-studied both in solution^{51,52} and in the gas phase,⁵³ due in part for its central role in lectin affinity chromatography.⁵⁴ Beyond its well-understood structure, the affinities of the four carbohydrate binding sites on Con A (one per monomer) are well known for a variety of manosyl carbohydrate ligands.^{55,56} The complex bound to many of these carbohydrates has been studied intact by MS,⁵³ as has its structural transitions as a function of solvent composition.⁵⁷ Cooperative binding models for the assembly have been discussed in the literature,^{58,59} but the extent of the cooperativity observed, and how that varies as a function of carbohydrate ligand, is currently relatively unknown. Our IM-MS and CIU data for Con A, which we acquired comprehensively over a range of carbohydrate ligands and binding stoichiometries, reveals evidence for differential cooperative stabilization that favors larger ligands. We discuss our methods and alternative explanations for our observations, as well as their potential implications for IM-MS, CIU and structural biology in general.

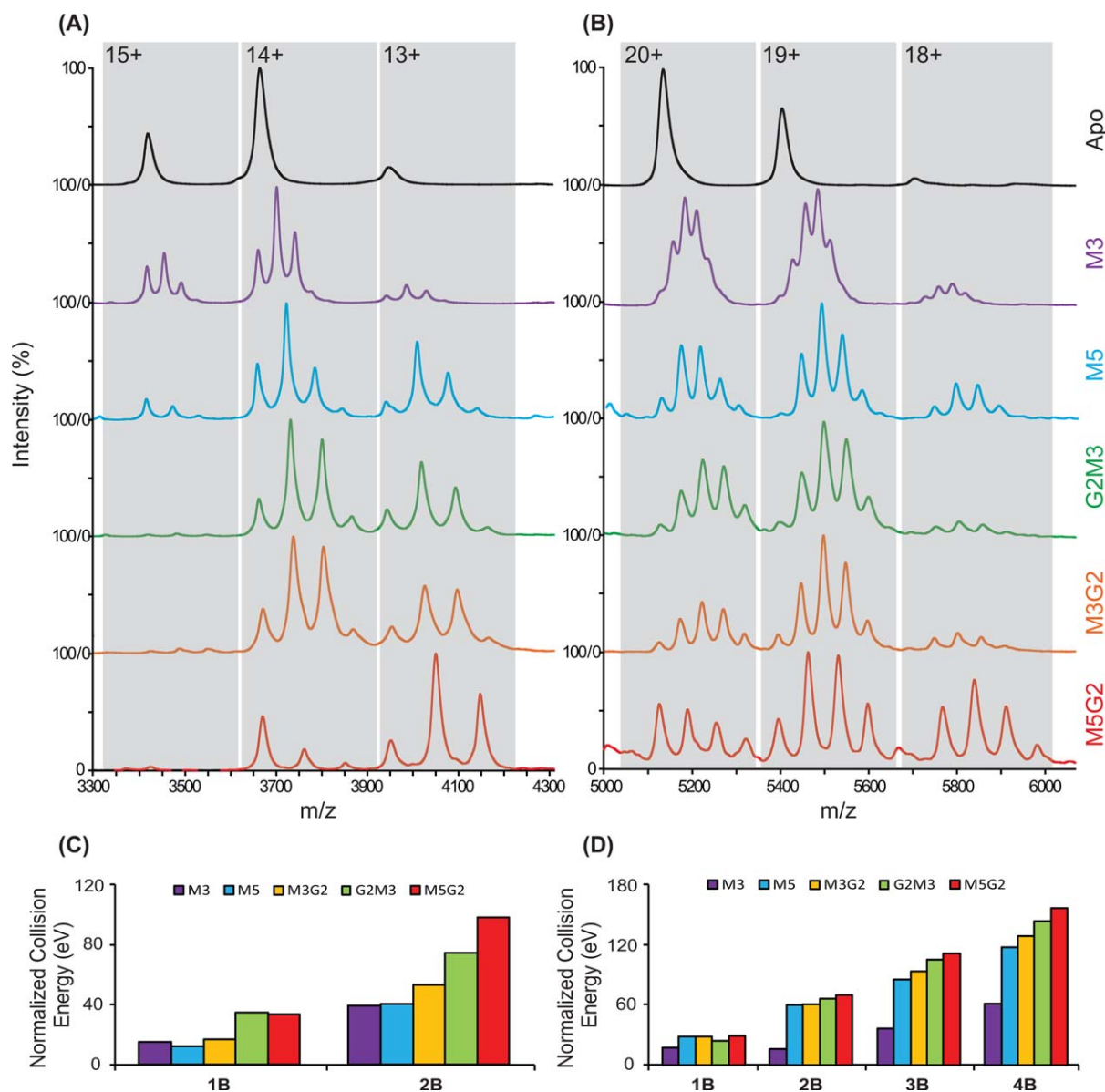


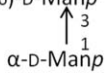
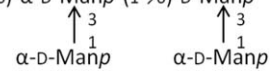
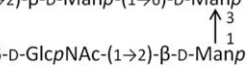
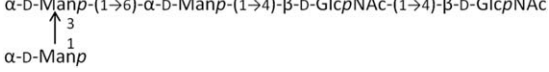
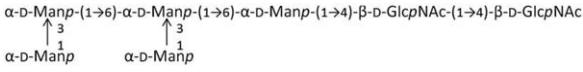
Figure 1. MS results for (A) dimeric and (B) tetrameric Con A incubated with all five carbohydrate ligands shown in Table I. CIU stability responses associated with each ligand bound states, across all protein charge states, are summarized in (C) and (D) for Con A dimers and tetramers, in terms of a laboratory collision energy (eV) normalized to that of the apo state. The presented CIU outputs are averaged from multiple charge states and normalized relative to the CIU stabilities recorded for apo Con A.

Results and Discussion

Figure 1(A,B) shows nESI-MS results for dimeric and tetrameric Con A incubated with all five of the carbohydrate ligands shown in Table I. For dimeric Con A, we observe largely apo, 1:1 and 1:2 Con A-ligand stoichiometries, with small amounts of non-specific 1:3 complexes detected due to excess ligand added in solution. Similarly, we observe resolved MS signals for apo, 1:1, 1:2, 1:3, and 1:4 Con A tetramer-ligand complexes, with negligible evidence of any nonspecific interactions and having integrated intensity values (over all charge states) that correlate well with expected K_D values.^{32,33} Furthermore, we note that the relative intensities of the bound states observed favor higher ligand occupancies

more strongly for lower protein charge states, as observed previously,⁵³ an observation most-likely linked to differences in the kinetic and internal energies of the Con A ions as a function of charge state. In general, manosyl carbohydrate ligands, which are ranked in increasing size and binding affinity (top to bottom), show concomitant increases in the bound population observed when ligand concentration is kept constant. Under our conditions, we found that the M3 ligands (504 Da) bound to the Con A tetramer represented the practical limits of our MS resolving power, as shown in Figure 1(B). Similarly, excess M5G2 (1235 Da) binding can cause MS overlap between the 19+ and 20+ signal clusters in Figure 1(B). By tuning the molar ratio

Table I. Carbohydrate Ligands, Their Correlated Abbreviations, Molecular Mass, and Dissociation Constants (K_D) Relative to the Concanavalin A Tetramer

Structure	Abbr.	M_w (Da)	K_D (μM) ^a
$\alpha\text{-D-Manp-(1}\rightarrow\text{6)-D-Manp}$ 	M3	504.4	2.97
$\alpha\text{-D-Manp-(1}\rightarrow\text{6)-}\alpha\text{-D-Manp-(1}\rightarrow\text{6)-D-Manp}$ 	M5	828.7	2.85, 1.51
$\beta\text{-D-GlcpNAc-(1}\rightarrow\text{2)-}\beta\text{-D-Manp-(1}\rightarrow\text{6)-D-Manp}$ 	G2M3	910.8	0.71
$\alpha\text{-D-Manp-(1}\rightarrow\text{6)-}\alpha\text{-D-Manp-(1}\rightarrow\text{4)-}\beta\text{-D-GlcpNAc-(1}\rightarrow\text{4)-}\beta\text{-D-GlcpNAc}$ 	M3G2	910.8	0.77
$\alpha\text{-D-Manp-(1}\rightarrow\text{6)-}\alpha\text{-D-Manp-(1}\rightarrow\text{6)-}\alpha\text{-D-Manp-(1}\rightarrow\text{4)-}\beta\text{-D-GlcpNAc-(1}\rightarrow\text{4)-}\beta\text{-D-GlcpNAc}$ 	M5G2	1235.1	0.32

^a All K_D values are derived from previous data.⁵³ In cases where multiple K_D values are reported for the same carbohydrate ligand, they are reported from Mandal *et al.*⁶⁰

between ligand and protein used during our experiments, we were able to optimize our MS signal to the extent where such overlaps were minimized.

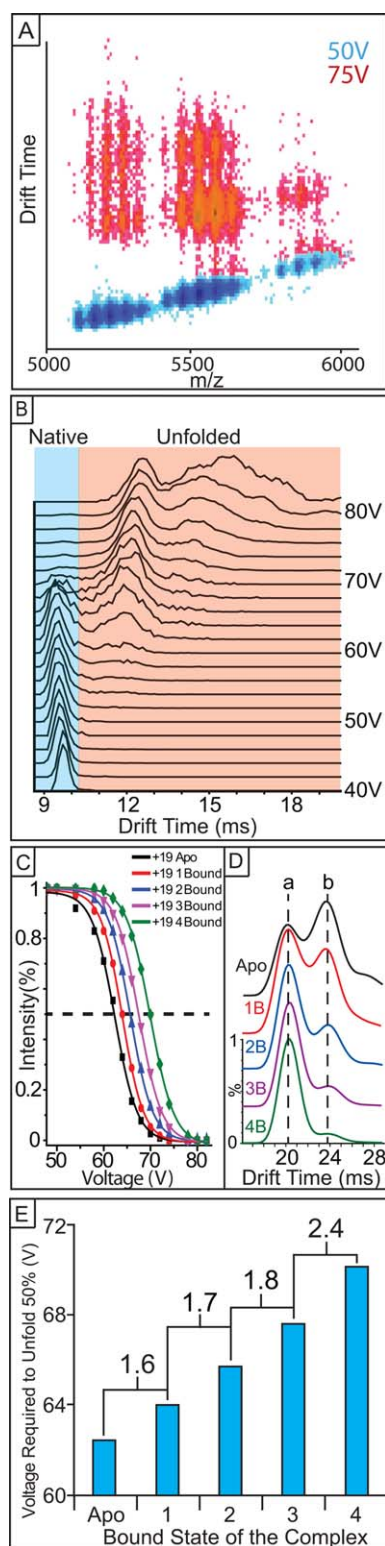
CIU data was recorded for each of the signals observed in Figure 1(A,B), and the CIU stabilities associated with each of these ligand bound states are summarized in Figure 1(C,D) for Con A dimers and tetramers, respectively, displayed as a normalized laboratory frame collision energy averaged over all all charge states observed.⁴⁵ The CIU outputs shown are averaged from multiple charge states and normalized relative to the CIU stabilities recorded for apo Con A. Results show that when carbohydrates interact with either dimeric or tetrameric Con A, the stability of the assembly is generally enhanced. In addition, our CIU stabilities do not possess a strong correlation with either the molecular mass or the solution-phase K_D values for the ligands assessed (Supporting Information Fig. S1). The stability enhancements observed in our CIU measurements cover a broad a range. For example, by comparing apo and 1:4 tetramer–ligand complexes, we measure a stability enhancement of 101.5 eV (laboratory frame energy) for M5G2 complexes when compared to those composed of M3-bound Con A. It is worth noting that all of the carbohydrate ligands tested in this report contain a tri-mannose core structure previously observed to interact with high affinity with Con A.^{58,60} As reference, we tested a number of ligands that lacked this tri-mannose structure and observed no evidence of ligand binding, in a similar fashion to previous data.^{56,58}

To ascertain the information content of our IM-MS and CIU data relative to the stabilities of the Con A–ligand complexes obtained through conventional MS measurements, collision induced dissociation

(CID) stabilities were also recorded for all signals observed in Figure 1(A, B) and compared to those generated from CIU. As discussed previously,^{34,35} CID stabilities can be extracted from MS data in a similar manner to the CIU stability values that are extracted from IM data (see Fig. 2) and correspond to the collision energy required to dissociate 50% of the bound ligand from the intact Con A–ligand assembly. For example, CID and CIU stabilities are recorded and compared for Con A–M3G2 complexes in Figure 3, and these data are representative of all similar comparisons that we conducted comprehensively throughout our Con A–ligand complex dataset (data not shown). While uniform CID stabilities are recorded for all ions, we observe significant differential effects on protein stability by CIU, varying by 13% over the apo to 1:4 Con A tetramer–ligand complexes detected. Similar disparities between CID and CIU stability values have been observed for tetrameric transthyretin–thyroxine complexes, with CIU results indicating significant stability differences both between bound states and mutant forms of the protein, whereas CID only detected stability differences upon protein mutation.³⁵

In addition to detecting stability enhancements upon ligand binding that are not apparent using CID, CIU detects significant differences in the stability conferred to Con A upon ligand binding that, upon close inspection, appears nonlinear with respect to Con A ligand occupancy. Figure 4(A) shows CIU stability values for M3 and M5 bound to the 20+ charge state of the Con A tetramer. As discussed above, increasing levels of ligand occupancy enhances the stability of the resulting Con A complex. However, Figure 4(B), which plots the collision

voltage differences recorded between adjacent Con A bound states for M3 and M5, reveals significant non-linear increases in stability for M5 that are not apparent for M3. For example, upon transitioning from a 1:1 to a 1:2 Con A tetramer: ligand complex, M3 binding allows the assembly to survive for an additional 0.9 V, while M5 binding adds 1.4 V of stability enhancement, despite both ligands conferring



nearly identical stability increases upon transition from apo to 1:1 complex forms. Similar to 1:2 complexes, M5 binding shifts CIU stability by 2.2 V, whereas 1.1 V of stability are added to CIU data for M3, when 1:4 Con A tetramer:ligand complexes are considered. Conversely, 1:3 complexes generated with either ligand generate similar enhancements in tetramer CIU stability. Both of the stability differences cited above, for 1:2 and 1:4 complexes, are outside of the computed standard deviation derived error bars (ranging between 0.1 and 0.3 V) for our relative CIU comparison plots. Overall, the data presented in Figure 4(B) clearly supports a positively cooperative stability enhancement in the Con A tetramer upon binding M5, congruent with known Con A structure and ligand binding mechanisms.⁵⁸ Similar data analysis was performed in M5G2 and M3G2, also revealing evidence of cooperative stabilization (Supporting Information Fig. S2), leaving M3 as the only carbohydrate ligand for which no cooperative enhancements in CIU stability are detected.

To compare our gas-phase CIU results with direct measurements of cooperative binding in solution, we performed isothermal titration calorimetry (ITC) assays on approximately 500 μM Con A samples incubated with three carbohydrate binders (M3, M5, G2M3). Supporting Information Figure S3 plots the enthalpy change recorded by ITC against the number of sample injections performed, which is correlated with carbohydrate ligand concentration. Recorded isotherms for all three Con A-carbohydrate complexes exhibit a “U” shaped profile, instead of a sigmoid, indicative of positive binding cooperativity.⁵⁸ Further attempts were made to differentiate and rank the cooperative binding observed. For example, we plotted the fractional saturation ratio of Con A against the free carbohydrate ligand

Figure 2. Experimental protocol for measuring the gas-phase stabilities of Con A-carbohydrate complexes. (A) Protein ions are first generated by nanoESI, and different binding stoichiometries are identified by MS. Representative data at activation voltages of 50 V (blue) and 75 V (red) are shown and exhibit different extents of collisional unfolding. (B) The IM drift time signals are further isolated according to the m/z values corresponding to each ligand bound species detected and analyzed as a function of activation voltage (shown as a IM drift time stack plot). (C) The percentage of compact Con A complex ions observed is computed at each charge state, and each activation voltage, ranging from apo to all carbohydrate-bound species. (D) Representative IM drift time stack plots of protein CIU response as a function of ligand binding. The relative population shift from structural family b to a upon ligand binding is related to the stability conferred to the Con A complex upon ligand binding. (E) Histograms captured at 50% intensity thresholds shown in (C) are generated, which quantify the relative collision voltage required to unfold 50% of the selected protein complex ions. Differential CIU stabilities extracted for proximal bound states are also calculated for our cooperative stabilization analysis.

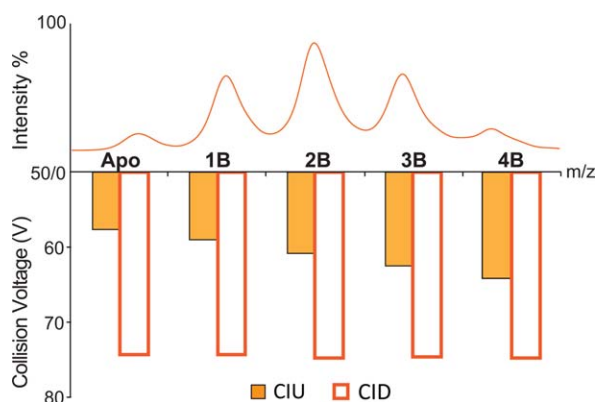


Figure 3. Representative MS results (top) and histograms (bottom) revealing the collision energy required for 50% unfold/dissociation of the 20+ Con A complexes (as labeled), each having different numbers of bound M3G2. The ability to detect differential stabilization upon ligand binding, and thus any cooperative stabilization effect, is unique to our CIU measurements, as no significant differences in MS bound state intensity or CID stability are detected.

concentration (data not shown), but this analysis resulted in similar values for the relative cooperativity of all ligands tested. Typically, the magnitude of the binding cooperativity detected is strongly reliant upon ligand binding affinity.^{61,62} The ligands chosen for our ITC screen all exhibit similar K_D values relative to Con A, in agreement with this general observation (see Table I). CIU results do not detect any cooperative stabilization upon M3 binding to Con A, despite evidence of a cooperative binding mechanism in solution. This observation may be due to the relatively small mass (504.4 Da) and weak affinity ($K_D = 2.97 \mu M$) of M3 relative to the other carbohydrates studied here. Alternatively, cooperative stabilization of Con A might not necessarily be linked with cooperative binding, as few examples exist in the literature where both values are probed simultaneously through experiment. Regardless, CIU and ITC results both detect cooperative stabilization and binding, respectively, for the other carbohydrate ligands studied here, providing clear evidence of a potential correlation between gas-phase Con A structure and stability and solution-phase protein function.

Still deeper analysis of CIU data provides a more comprehensive picture of the stabilization mechanism adopted by Con A-carbohydrate ligand complexes, as well the potential limitations surrounding the detection of the cooperative stabilization effects described above. Figure 4(C) shows a comparison of the relative differences in CIU stability recorded for 19+ Con A complex ions in comparison with 20+ ions, where the latter ions and their stabilities are described in detail above [Figure 4(A,B)]. While strong cooperative stabilization of Con A is observed for M5 bound complexes when

20+ ions are analyzed, little evidence of positive cooperativity is observed in the CIU data for 19+ Con A-M5 complex ions. We rationalize this result based on the likely differential ion temperature and energetics of the 19+ and 20+ Con A complexes. It has been observed previously that the CIU and collisional remodeling of protein complexes is highly charge state dependant.^{35,44,45,50} As such, it is not surprising that cooperative stabilization cannot be detected throughout all Con A-ligand complex charge states, as these ions likely possess different threshold energies for collisional unfolding and do so via different mechanistic pathways. Additional pathway details are available through the use of CIU “fingerprints” which track the size of the Con A complex as a function of the collision voltages used to initiate CIU. These data (Supporting Information

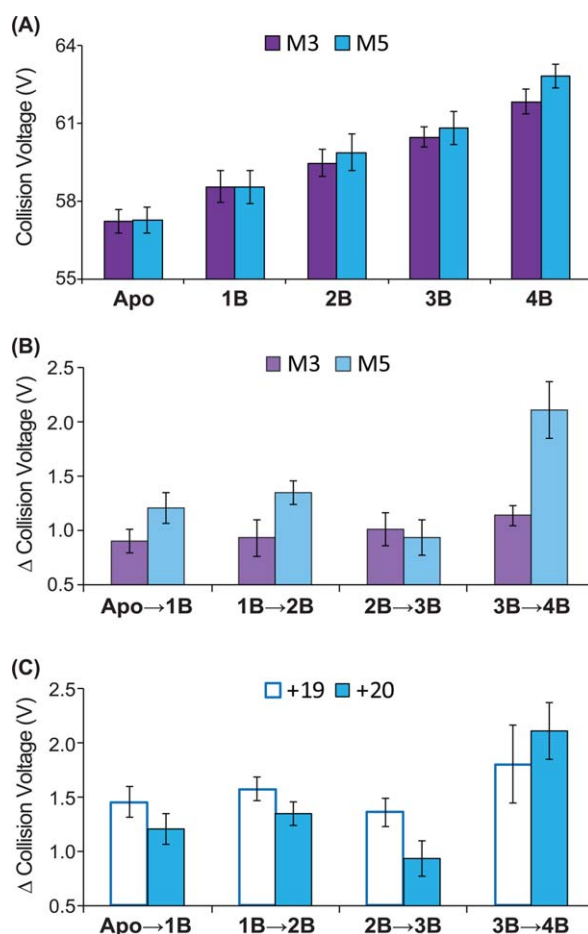


Figure 4. (A) CIU stability responses for ligand M3 (purple) and M5 (blue) bound to the 20+ charge state of Con A tetramer. (B) Collision voltage differences recorded between adjacent Con A bound state for ligand M3 and M5. Data indicates significant nonlinear stability increment for M5 that are not apparent for M3. (C) CIU-based collision voltage difference values for M5 bound Con A complexes recorded for 19+ (open blue box) and 20+ (filled blue box) ions. The cooperative stabilization effect observed is clear for those ions having a higher overall charge but not apparent for those of lesser charge state.

Fig. S4) strongly indicate that the presence of the bound ligand does not alter the unfolding pathway of the Con A tetramer, when compared with control fingerprints acquired for the Apo protein. Instead, global stabilization of Con A relative to CIU (for both the 19+ and 20+ ions) occurs through an increased stability of the most compact form of the assembly (Supporting Information Fig. S5, S6). Since such compact forms of the protein are more closely linked to the native state structure of Con A,³⁵ such results link more closely the cooperative stabilization effects observed to potential analogous stabilization upon Con A–carbohydrate binding in solution.

Experimental Methods

Sample preparation

Con A was purchased from Sigma (St. Louis, MO), and associated mannosyl carbohydrate ligand systems were purchased from V-LABS (Covington, LA). Con A is a lectin mannosyl carbohydrate-binding protein tetramer, with well-studied sequence and structure.⁵² Con A contains one carbohydrate binding site per protein subunit, with each monomer consisting of 237 amino acids ($M_w = 25.7$ kDa), arranged into two antiparallel β -sheets. While the biological unit of the complex is a tetramer, the assembly has an established pH-dependent equilibrium with a dimeric form, with the dimer dominating below pH 5.6 and at low temperatures.⁶³ Con A has a high affinity to glucose/mannose carbohydrates and exhibits the highest affinity for carbohydrates having a tri-mannoside, 3,6-di-*O*-(α -D-mannopyranosyl)-D-mannose core.^{55,60} The Con A carbohydrate binding site is situated on a solvent exposed cap of each monomeric unit, proximal to two metal binding sites; a transition metal ion site (S1, typically Mn^{2+}) and a Ca^{2+} site (S2).⁶⁴ It has been reported that dimeric and tetrameric Con A bind similarly to a variety of carbohydrates, as reported by both calorimetry⁵⁸ and nESI-MS.⁵³ We have chosen five oligosaccharide ligands with different binding affinities, having K_D s ranging from 0.32 to 2.97 μM and molecular weights ranging from 504 to 1235 Da (See Table I for details), to evaluate the CIU responses for Con A.

Ion mobility-mass spectrometry

Protein–ligand samples (~ 10 μL) were analyzed using our quadrupole IM time-of-flight MS instrument (Synapt G2 HDMS, Waters, Milford, MA). Complex ions were generated using a nESI source and optimized to allow transmission of protein–ligand complexes. The capillary voltage of the nESI source was typically held around 1.6 kV, with the source operating in positive mode. The sampling cone was operated at approximately 90 V. The traveling-wave IM separator was operated at an N_2

pressure of approximately 3.5 mbar, using a 40 V wave amplitude traveling at 800–1000 ms^{-1} , to generate IM separation. Protein samples were prepared in 100 mM ammonium acetate at pH 7 to a concentration of 10 μM following buffer exchange. Saccharide ligand samples were also prepared in aqueous solution at concentrations of 10 μM using 100 mM ammonium acetate buffer concentrations. All ligands were incubated with Con A for 30 min prior to nESI-IM-MS analysis.

Collision induced unfolding measurements

Collisional activation in the ion trap traveling-wave ion guide prior to the IM separator was used for CIU of protein complexes to investigate the gas-phase stability of protein ions bound to different carbohydrate ligands. Experiments were initially performed in tandem-MS mode. Ions were selected in the quadrupole mass filter at an m/z corresponding to the 19+ and 20+ charge state of Con A bound to different ligands. Results showed that carbohydrate ligands bind tightly to Con A under our experimental conditions, with no apparent ligand dissociation and charge stripping (up to 9% signal lost for 19+ and 13% for 20+, at trap collision energy of 100 V). Data were then collected under a high-throughput native MS1 mode, where we transmitted all ligand bound states simultaneously into the ion trap, to undergo CIU simultaneously. CIU data were acquired by varying the trap collision voltage experienced by ions as they enter the ion trap region of the instrument in 2–5 V increments and recording IM data for MS-isolated peaks at each discrete voltage value.

Data analysis

All mass spectra were processed with Masslynx 4.1 software (Waters). The relative intensities of compact Con A tetramer/dimer ions for both apo and ligand bound species (I_f), the only features observed when no activation energy was applied, were calculated as a percentage of the total ion intensity observed at a selected m/z value corresponding to the intact corresponding tetramer or dimer ions using Eq. (1). This value is used to chart the unfolding process of protein oligomers as a function of activation voltage used throughout our dataset. The typical standard deviation for the determination of I_f (%) was 2–4%.

$$I_f(\%) = \frac{I_{\text{folded}}}{\sum I_{\text{conformers}}} \times 100 \quad (1)$$

Figure 2 further demonstrates the typical experimental protocol we have developed for measuring the gas-phase stabilities of Con A–Carbohydrate complexes: Protein ions are first generated by nESI

and different binding stoichiometries are identified by MS, in the positive ion mode. When low activation voltages are used [blue data, Fig. 2(A)], all protein charge states and ligand bound states remain compact and monomodal with respect to their IM arrival time distributions. As the activation voltage is increased (shown in red), IM distributions increase in drift time and become multimodal, indicating protein unfolding in the gas phase. Prior to collecting complete datasets, we conducted preliminary surveys of the IM-MS data as a function of activation voltage to assess the course changes in IM drift time encountered by Con A over the activation voltage range available for CIU measurements. The IM drift time signals are further isolated according to the m/z values corresponding to each ligand bound species detected [Fig. 2(B)], and the percentage of compact Con A complex ions observed is computed at each activation voltage used for CIU data collection [Fig. 2(C)]. The resultant compact ion intensities are then plotted against a range of activation voltages, typically ranging from 20 to 100 V, for both the dimeric and tetrameric forms of the Con A–oligosaccharide complexes observed. When we compare protein CIU as a function of ligand binding, additional bound carbohydrates universally stabilize Con A [Fig. 2(D)]. To quantitatively evaluate the stabilizing influence of carbohydrate binding on Con A, histograms captured at the 50% intensity thresholds shown in Figure 2(C) are generated, which quantify the relative collisional energy required to unfold 50% of the selected protein complex ions [Fig. 2(E)]. CIU voltage differences captured at 50% relative ion intensity between two adjacent bound states are also calculated in order to assess potential cooperative increases in Con A stability [Fig. 2(E)].

Isothermal titration calorimetry

ITC measurements were performed on a nanoITC 2G model system from TA Instruments (Waters LLC, New Castle, DE). Briefly, 20 μM Con A and 500–600 μM carbohydrate ligand, both in 100 mM ammonium acetate buffer at pH 7, were used to achieve optimal isotherm titration curves. Blank buffer runs were performed for baseline determination prior to protein ligand titration experiments. Con A solutions were degassed for 15 min, taking care to avoid air bubble formation in the sample, before loading them into the calorimeter cell. The titrations were performed at 25°C, a 300 rpm stir rate, with a >1800 s equilibration time, and followed by 24 injections separate sample injections each with a 240 s spacing. Raw ITC data were analyzed by NanoAnalyze software and were exported to excel for further cooperativity analysis.

Conclusions

Here, we present evidence of the cooperative stabilization of a 103-kDa lectin protein tetramer upon

carbohydrate ligand binding. We use CIU, a novel MS-based methodology that has only been applied in a few cases, to make this assessment, and show that such stabilization cannot easily be detected using solution phase technologies (*e.g.*, ITC) or by MS alone. Indeed, such stability measurements require the separation of resolved ligand bound states of the protein complex to individually address the stability of each state in isolation. The IM-MS and CIU methods described here are uniquely able to accomplish this and generate stability data that can potentially be used to inform energy calculations aimed at assessing the details of such cooperative effects. We note a general agreement between our data, and cooperative binding data acquired in solution here, as well our general agreement with previous reports.^{53,58,61} We also note that weak correlations are found between CIU stability and ligand K_D values or molecular mass, demonstrating the orthogonality of CIU stability data and its likely dependence upon complex structure, as well as the mechanistic details of the CIU process.

It is clear, however, that caveats exist for the trends reported here. First, cooperativity is most apparent in higher charge states for the Con A complexes observed. Previous data has linked lower charge states more closely to native-state protein structures.^{35,65} but has also discovered clear CIU dependencies upon protein charge state that connect to the overall mechanism of activation-initiated gas-phase protein unfolding and remodeling. In addition, small ligands (*e.g.*, M3) do not exhibit cooperative stabilization effects in our CIU dataset but do exhibit cooperative binding in solution (Supporting Information Fig. S2). This discrepancy likely stems directly from the CIU process, which may discriminate against small, weak binders that cannot remain bound to the protein in large numbers following collisional activation. Despite these minor caveats, however, the CIU data shown here adds substantially to the growing list of applications that such gas-phase experiments have found, which currently includes: stability assessments of protein–cation/anion complexes,^{45,66} the discovery of conformationally selective kinase inhibitors,⁵⁰ and the assignment of membrane protein–lipid binding modes.⁴⁴ It is clear that future work will continue to expand the CIU experiment to more experiments that use its unique ability to extract protein stability values from complex protein mixtures, using relatively small amounts of sample.

References

1. Williams DH, Stephens E, O'Brien DP, Zhou M (2004) Understanding noncovalent interactions: ligand binding energy and catalytic efficiency from ligand-induced reductions in motion within receptors and enzymes. *Angew Chem-Int Ed* 43:6596–6616.

2. Eaton WA, Henry ER, Hofrichter J, Mozzarelli A (1999) Is cooperative oxygen binding by hemoglobin really understood? *Nat Struct Mol Biol* 6:351–358.
3. Pantoliano MW, Horlick RA, Springer BA, Vandyk DE, Tobery T, Wetmore DR, Lear JD, Nahapetian AT, Bradley JD, Sisk WP (1994) Multivalent ligand-receptor binding interactions in the fibroblast growth-factor system produce a cooperative growth-factor and heparin mechanism for receptor dimerization. *Biochemistry* 33:10229–10248.
4. Wyman J (1964) Linked functions and reciprocal effects in hemoglobin: a second look. *Adv Protein Chem* 19:91.
5. Li R, Botchan MR (1993) The acidic transcriptional activation domains of VP16 and p53 bind the cellular replication protein A and stimulate in vitro BPV-1 DNA replication. *Cell* 73:1207–1221.
6. Myers RM, Rio DC, Robbins AK, Tjian R (1981) SV40 gene expression is modulated by the cooperative binding of T antigen to DNA. *Cell* 25:373–384.
7. Martin A, Baker TA, Sauer RT (2005) Rebuilt AAA+ motors reveal operating principles for ATP-fuelled machines. *Nature* 437:1115–1120.
8. Katz DH, Hamaoka T, Benacerraf B (1973) Cell interactions between histoincompatible T and B lymphocytes II. Failure of physiologic cooperative interactions between T and B lymphocytes from allogeneic donor strains in humoral response to hapten-protein conjugates. *J Exp Med* 137:1405–1418.
9. McGhee JD, von Hippel PH (1974) Theoretical aspects of DNA-protein interactions: co-operative and non-cooperative binding of large ligands to a one-dimensional homogeneous lattice. *J Mol Biol* 86:469–489.
10. Zhao Y-L, Wu Y-D (2002) A theoretical study of β -sheet models: is the formation of hydrogen-bond networks cooperative? *J Am Chem Soc* 124:1570–1571.
11. Murphy KP, Freire E (1992) Thermodynamics of structural stability and cooperative folding behavior in proteins. *Adv Prot Chem* 43:313–361.
12. Stam JC, Sander EE, Michiels F, van Leeuwen FN, Kain HE, van der Kammen RA, Collard JG (1997) Targeting of Tiam1 to the plasma membrane requires the cooperative function of the N-terminal pleckstrin homology domain and an adjacent protein interaction domain. *J Biol Chem* 272:28447–28454.
13. Kindon H, Pothoulakis C, Thim L, Lynch-Devaney K, Podolsky DK (1995) Trefoil peptide protection of intestinal epithelial barrier function: cooperative interaction with mucin glycoprotein. *Gastroenterology* 109:516–523.
14. Looger LL, Dwyer MA, Smith JJ, Hellinga HW (2003) Computational design of receptor and sensor proteins with novel functions. *Nature* 423:185–190.
15. Mizoue LS, Chazin WJ (2002) Engineering and design of ligand-induced conformational change in proteins. *Curr Opin Struct Biol* 12:459–463.
16. Duke TAJ, Le Novere N, Bray D (2001) Conformational spread in a ring of proteins: a stochastic approach to allostery. *J Mol Biol* 308:541–553.
17. Miller DW, Dill KA (1997) Ligand binding to proteins: the binding landscape model. *Protein Sci* 6:2166–2179.
18. Feng J, Walter NG, Brooks CL (2011) Cooperative and directional folding of the preQ(1) Riboswitch aptamer domain. *J Am Chem Soc* 133:4196–4199.
19. Alexander P, Fahnestock S, Lee T, Orban J, Bryan P (1992) Thermodynamic analysis of the folding of the streptococcal protein-G IgG-binding domains B1 and B2—why small proteins tend to have high denaturation temperatures. *Biochemistry* 31:3597–3603.
20. Freire E (1999) The propagation of binding interactions to remote sites in proteins: analysis of the binding of the monoclonal antibody D1.3 to lysozyme. *Proc Natl Acad Sci USA* 96:10118–10122.
21. Street TO, Krukenberg KA, Rosgen J, Bolen DW, Agard DA (2010) Osmolyte-induced conformational changes in the Hsp90 molecular chaperone. *Protein Sci* 19:57–65.
22. Dyachenko A, Gruber R, Shimon L, Horovitz A, Sharon M (2013) Allosteric mechanisms can be distinguished using structural mass spectrometry. *Proc Natl Acad Sci* 110:7235–7239.
23. DeChancie J, Houk K (2007) The origins of femtomolar protein–ligand binding: hydrogen-bond cooperativity and desolvation energetics in the biotin–(strept) avidin binding site. *J Am Chem Soc* 129:5419–5429.
24. Marcos E, Crehuet R, Bahar I (2011) Changes in dynamics upon oligomerization regulate substrate binding and allostery in amino acid kinase family members. *PLoS Comput Biol* 7.
25. Rosengarth A, Rosgen J, Hinz HJ, Gerke V (2001) Folding energetics of ligand binding proteins II. Cooperative binding of Ca^{2+} to annexin I. *J Mol Biol* 306:825–835.
26. Doyle ML, Gill SJ, Cusanovich MA (1986) Ligand-controlled dissociation of chromatium-*vinosum* cytochrome-C'. *Biochemistry* 25:2509–2516.
27. Loo JA (1997) Studying noncovalent protein complexes by electrospray ionization mass spectrometry. *Mass Spectrom Rev* 16:1–23.
28. Robinson CV, Chung EW, Kragelund BB, Knudsen J, Aplin RT, Poulsen FM, Dobson CM (1996) Probing the nature of noncovalent interactions by mass spectrometry. A study of protein–CoA ligand binding and assembly. *J Am Chem Soc* 118:8646–8653.
29. Niu S, Rabuck JN, Ruotolo BT (2013) Ion mobility-mass spectrometry of intact protein–ligand complexes for pharmaceutical drug discovery and development. *Curr Opin Chem Biol* 17:809–817.
30. Hyung SJ, Ruotolo BT (2012) Integrating mass spectrometry of intact protein complexes into structural proteomics. *Proteomics* 12:1547–1564.
31. Cheng KW, Wong CC, Wang MF, He QY, Chen F (2010) Identification and characterization of molecular targets of natural products by mass spectrometry. *Mass Spectrom Rev* 29:126–155.
32. Wang WJ, Kitova EN, Klassen JS (2003) Influence of solution and gas phase processes on protein–carbohydrate binding affinities determined by nano-electrospray Fourier transform ion cyclotron resonance mass spectrometry. *Anal Chem* 75:4945–4955.
33. Sun JX, Kitova EN, Wang WJ, Klassen JS (2006) Method for distinguishing specific from nonspecific protein–ligand complexes in nano-electrospray ionization mass spectrometry. *Anal Chem* 78:3010–3018.
34. Ruotolo BT, Hyung SJ, Robinson PM, Giles K, Bateman RH, Robinson CV (2007) Ion mobility–mass spectrometry reveals long-lived, unfolded intermediates in the dissociation of protein complexes. *Angew Chem Int Ed* 46:8001–8004.
35. Hyung S-J, Robinson CV, Ruotolo BT (2009) Gas-phase unfolding and disassembly reveals stability differences in ligand-bound multiprotein complexes. *Chem Biol* 16:382–390.
36. Benesch JL, Ruotolo BT (2011) Mass spectrometry: come of age for structural and dynamical biology. *Curr Opin Struct Biol* 21:641–649.
37. Strickland EC, Geer MA, Tran DT, Adhikari J, West GM, DeArmond PD, Xu Y, Fitzgerald MC (2013)

- Thermodynamic analysis of protein–ligand binding interactions in complex biological mixtures using the stability of proteins from rates of oxidation. *Nat Protoc* 8:148–161.
38. Zhang Q, Chen J, Kuwajima K, Zhang HM, Xian F, Young NL, Marshall AG (2013) Nucleotide-induced conformational changes of tetradecameric GroEL mapped by H/D exchange monitored by FT-ICR mass spectrometry. *Sci Rep* 3.
 39. van Duijn E, Bakkes PJ, Heeren RM, van den Heuvel RH, van Heerikhuizen H, van der Vies SM, Heck AJ (2005) Monitoring macromolecular complexes involved in the chaperonin-assisted protein folding cycle by mass spectrometry. *Nat Methods* 2:371–376.
 40. Monod J, Wyman J, Changeux J-P (1965) On the nature of allosteric transitions: a plausible model. *J Mol Biol* 12:88–118.
 41. Changeux JP (2012) Allostery and the Monod-Wyman-Changeux model after 50 years. *Annu Rev Biophys* 41:103–133.
 42. Hopper JT, Oldham NJ (2009) Collision induced unfolding of protein ions in the gas phase studied by ion mobility-mass spectrometry: the effect of ligand binding on conformational stability. *J Am Soc Mass Spectrom* 20:1851–1858.
 43. Zhu F, Lee S, Valentine SJ, Reilly JP, Clemmer DE (2012) Mannose7 glycan isomer characterization by IMS-MS/MS analysis. *J Am Soc Mass Spectrom* 23:2158–2166.
 44. Laganowsky A, Reading E, Allison TM, Ulmschneider MB, Degiacomi MT, Baldwin AJ, Robinson CV (2014) Membrane proteins bind lipids selectively to modulate their structure and function. *Nature* 510:172–175.
 45. Han L, Hyung S-J, Mayers JJ, Ruotolo BT (2011) Bound anions differentially stabilize multiprotein complexes in the absence of bulk solvent. *J Am Chem Soc* 133:11358–11367.
 46. Kanu AB, Dwivedi P, Tam M, Matz L, Hill HH (2008) Ion mobility–mass spectrometry. *J Mass Spectrom* 43:1–22.
 47. Jung JE, Pierson NA, Marquardt A, Scheffner M, Przybylski M, Clemmer DE (2011) Differentiation of compact and extended conformations of Di-ubiquitin conjugates with lysine-specific isopeptide linkages by ion mobility-mass spectrometry. *J Am Soc Mass Spectrom* 22:1463–1471.
 48. Han L, Ruotolo BT (2013) Traveling-wave ion mobility-mass spectrometry reveals additional mechanistic details in the stabilization of protein complex ions through tuned salt additives. *Int J Ion Mobil Spectrom* 16:41–50.
 49. Han L, Hyung S-J, Ruotolo BT (2013) Dramatically stabilizing multiprotein complex structure in the absence of bulk water using tuned Hofmeister salts. *Faraday Discuss* 160:371–388.
 50. Rabuck JN, Hyung S-J, Ko KS, Fox CC, Soellner MB, Ruotolo BT (2013) Activation state-selective kinase inhibitor assay based on ion mobility-mass spectrometry. *Anal Chem* 85:6995–7002.
 51. Lis H, Sharon N (1986) Lectins as molecules and as tools. *Ann Rev Biochem* 55:35–67.
 52. Bittiger H, Schnebli HP (1976) *Concanavalin A as a Tool*. New York: Wiley
 53. van Dongen WD, Hack AJR (2000) Binding of selected carbohydrates to apo-concanavalin A studied by electrospray ionization mass spectrometry. *Analyst* 125:583–589.
 54. Lotan R, Nicolson GL (1979) Purification of cell membrane glycoproteins by lectin affinity chromatography. *Biochim Biophys Acta* 559:329–376.
 55. Mandal DK, Kishore N, Brewer CF (1994) Thermodynamics of lectin-carbohydrate interactions. Titration microcalorimetry measurements of the binding of N-linked carbohydrates and ovalbumin to concanavalin A. *Biochemistry* 33:1149–1156.
 56. Dam TK, Roy R, Das SK, Oscarson S, Brewer CF (2000) Binding of multivalent carbohydrates to concanavalin A and Dioclea grandiflora lectin—Thermodynamic analysis of the "multivalency effect". *J Biol Chem* 275:14223–14230.
 57. Edelman GM, Cunningham BA, Reeke GN, Becker JW, Waxdal MJ, Wang JL (1972) The covalent and three-dimensional structure of concanavalin A. *Proc Natl Acad Sci USA* 69:2580–2584.
 58. Chervenak MC, Toone EJ (1995) Calorimetric analysis of the binding of lectins with overlapping carbohydrate-binding ligand specificities. *Biochemistry* 34:5685–5695.
 59. Zeng X, Andrade CA, Oliveira MD, Sun X-L (2012) Carbohydrate–protein interactions and their biosensing applications. *Anal Bioanal Chem* 402:3161–3176.
 60. Mandal DK, Brewer CF (1993) Differences in the binding affinities of dimeric concanavalin A (including acetyl and succinyl derivatives) and tetrameric concanavalin A with large oligomannose-type glycopeptides. *Biochemistry* 32:5116–5120.
 61. Houtman JC, Brown PH, Bowden B, Yamaguchi H, Appella E, Samelson LE, Schuck P (2007) Studying multisite binary and ternary protein interactions by global analysis of isothermal titration calorimetry data in SEDPHAT: application to adaptor protein complexes in cell signaling. *Protein Sci* 16:30–42.
 62. Dam J, Schuck P (2005) Sedimentation velocity analysis of heterogeneous protein-protein interactions: sedimentation coefficient distributions $c(s)$ and asymptotic boundary profiles from Gilbert-Jenkins theory. *Biophys J* 89:651–666.
 63. Bhattacharyya L, Brewer CF (1990) Isoelectric focusing studies of concanavalin A and the lentil lectin. *J Chromatogr A* 502:131–142.
 64. Liener I. 2012. *The lectins: properties, functions, and applications in biology and medicine*, Elsevier.
 65. Pagel K, Hyung S-J, Ruotolo BT, Robinson CV (2010) Alternate dissociation pathways identified in charge-reduced protein complex ions. *Anal Chem* 82:5363–5372.
 66. Han L, Hyung SJ, Ruotolo BT (2012) Bound cations significantly stabilize the structure of multiprotein complexes in the gas phase. *Angew Chem* 124:5790–5793.